Arch. Metall. Mater. **64** (2019), 1, 95-102

DOI: 10.24425/amm.2019.126223

J. SOBOTA*#, K. RODAK**, M. NOWAK*

MICROSTRUCTURE AND PROPERTIES OF TIN BRONZES PRODUCED BY THE SPD METHOD

In this article the structural and mechanical properties of grain refinement of Cu-Sn alloys with tin content of 10%, 15% and 20% using the KOBO method have been presented. The direct extrusion by KOBO (name from the combination of the first two letters of the names of its inventors – A. Korbel and W. Bochniak) method employs, during the course of the whole process, a phenomenon of permanent change of strain travel, realized by a periodical, two-sided, plastic metal torsion.

Moreover the aim of this work was to study corrosion resistance. The microstructure investigations were performed using an optical microscope Olimpus GX71, a scanning electron microscope (SEM) and a scanning transmission electron microscope (STEM). The mechanical properties were determined with INSTRON 4505/5500 machine. Corrosion tests were performed using «Autolab» set – potentiostat/galvanostat from EcoChemie B.V. with GPES software ver. 4.9. The obtained results showed possibility of KOBO deformation of Cu-Sn casting alloys. KOBO processing contributed to the refinement of grains and improved mechanical properties of the alloys. The addition of tin significantly improved the hardness. Meanwhile, with the increase of tin content the tensile strength and yield strength of alloys decrease gradually. Ductility is controlled by eutectoid composition and especially δ phase, because they initiate nucleation of void at the particle/matrix interface. No significant differences in the corrosion resistance between cast and KOBO processed materials were found.

Keywords: tin bronzes, KOBO, microstructure, mechanical properties, corrosion

1. Introduction

The dynamic development of various sectors of industry impose the search of new materials with improved properties. Meanwhile the development of new methods of plastic deformation renders production of well known materials with completely new properties possible. Nowadays, techniques of severe plastic deformations (SPD) are frequently used. The main aim of the SPD techniques is to increase mechanical and physical properties of metals and alloys through a significant grain size refinement [1-4]. Moreover, SPD very often is recognized as a potential tool for superplastic deformation. The obtained results confirm potential for achieving superplasticity at relatively low temperatures through grain refinement to the submicrometer level [3,4]. The formation of ultra-fine grained (UFG) microstructure by KOBO processing have been investigated more intensively. This method has been applied to a wide range of metals, alloys and composites [5-7]. KOBO belongs to methods with cyclic changes in the strain path. For this reason the diffusion of vacancies became quicker, resulting in the annihilation of dislocations by climbs. In contrast to conventional methods, in the direct extrusion by KOBO, in addition to parameters such as: extrusion temperature, speed, processing rate, batch geometry, it is possible to control other parameters of the deformation process. Thanks to this the properties of the product can be strictly controlled. Optimal conditions for the KOBO extrusion process provide possibilities for significant reduction of deformation work and less wear of working tools and, above all, deformation of difficult or even non-deformable materials. This technology allows you to obtain products in forms not available in traditional plastic working processes. [5]

In the results, the achievable saturation dislocation density is usually lower in cyclic methods than in monotonic [8,9]. KOBO processing is especially effective in introduction of extremely large deformation [5]. It is well known, that the character of the UFG microstructures depends on homologous temperature, chemical composition, value of stacking fault energy and additionally deformation parameters [10,11].

In this article we demonstrate the effectiveness of KOBO deformation as a technique for introduction of large strain deformation in Cu-Sn alloy (tin bronze).

Tin bronzes are oldest known alloys, used in the ancient times for production of swords, ornaments, dishes and everyday elements.

Tin bronzes for plastic working contain up to 9 [%wt.] of Sn, the rest is Cu with other elements. Above 9 [%wt.] of Sn, cold working of the tin bronzes becomes virtually impossible because of occurrence of eutectoid composition in the structure

* INSTITUTE OF NON – FERROUS METALS, 5 SOWIŃSKIEGO STR., 44-100 GLIWICE, POLAND
** SILESIAN UNIVERSITY OF TECHNOLOGY, FACULTY MATERIALS ENGINEERING AND METALLURGY, 8 KRASIŃSKIEGO STR., 40-019 KATOWICE, POLAND
# Corresponding author: joanna.sobota@imn.gliwice.pl

(Fig.1). Such alloys are known as casting bronzes. Casting bronzes are resistant to heavy constant and impact loads, corrosion and abrasion. Moreover, they show good castability and machinability [12-14].

The Cu-Sn phase diagram is complex (Fig. 1). Up to about 8%wt. of Sn in the alloys, single α phase is detected. Above 8%wt. of Sn, the microstructure consists of α phase and eutectoid composition ($\alpha + \delta$). The Cu-Sn equilibrium diagram shows a wide range of temperatures of α phase solidification. Significant temperature difference between the liquidus and solidus lines and low rate of tin diffusion in copper favor dendritic segregation, i.e. heterogeneity of the chemical composition within dendrites [13,14].

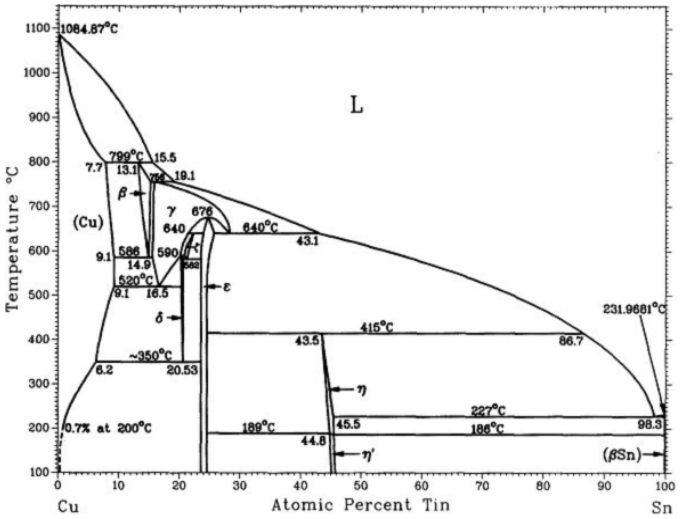

Fig. 1. Cu-Sn phase diagram

In the literature there are data about deformation of casting Cu-Sn alloys using the high pressure torsion (HPT) method [15,16]. The authors observed Cu matrix (α phase) in the CuSn7.8 alloy with uniformly dispersed precipitates of ε phase, while in the CuSn23 alloy the plates of ε phase and mixture of ($\alpha + \varepsilon$) phase were noticed. After HPT deformation, strong fragmentation of the α phase to nanometer range and partial dissolution of the ε phase in the Cu matrix in the CuSn7.8 alloy was observed [15]. In the alloy with tin content of 36%, the microstructure before deformation consists of coarse plates of ζ and ε phases (Hume-Rothery electron phases) [16]. After HPT processing, the density of dislocations increases in both phases. Moreover, cracks in the ε phase plates were observed. However, neither phase dissolution or phase transformation were observed [16]. Currently, Cu-Sn alloys after SPD processing are less studied, and this situation limits the areas of discussion.

In this article the structural and mechanical properties of grain refinement of Cu-Sn alloys with a tin content of 10%, 15% and 20% using the KOBO method have been presented. Moreover the aim of this work was to study corrosion resistance. It is very likely that these alloys can find new potential applications as dental tools or clamping dental screws.

2. Methodology, material for studies

The material for KOBO deformation was in the form of technical Cu-Sn alloy with 10%wt. of Sn (CuSn10), 15%wt.of Sn (CuSn15), and 20%wt. of Sn (CuSn20). Copper cathodes, metallic tin and small amounts of CuP alloy were used. The materials were melted in an induction furnace in graphite crucible. The melted CuSn10, CuSn15, CuSn20 alloys were cast (from a temperature of approx. 1150°C) into a round graphite ingot with a diameter of 50 mm, and allowed to cool down. After cooling, the ingots were removed from the moulds, their foot and head were cut out, and they were machined to 49.5 mm in diameter. In order to determine the composition of cast ingots, a semi-quantitative analysis of chemical composition of all produced materials was made. Studies of the chemical composition of alloys were performed by electrogravimetry (Cu determination) and atomic emission spectrometry using Horiba Yobin Yvon sequential emission spectrometer with excitation in inductively coupled plasma. The ingots were homogenized in an electric resistance furnace at 740°C for 24 hours to reduce tin segregation. KOBO processing was performed to the diameter of rods of 5 mm. The deformation tests were carried out with the modernized KOBO 2.5 MN horizontal hydraulic press at elevated temperature. Before deformation the samples were heated up in a resistance furnace in the temperature of 590°C with overpressure blow of protective gas. In this experiment nitrogen was applied. The recipient temperature was about 60°C. All tests were carried out at constant angle of rotation of the die, which was 8°. In all tests the die rotation frequency was 4 Hz. The microstructure has been analyzed by optical microscope Olimpus GX71, scanning electron microscope ZEISS LEO GEMINI 1525 and scanning transmission electron microscope (STEM) Hitachi HD-2300A. Additionally, qualitative analysis of the phase composition was performed. The qualitative analysis of the phase composition of the samples was performed with X-ray diffractometer XRD7 by Seifert-FPM.

The tensile tests were performed with INSTRON 4505/5500 machine at room temperature at an initial strain rate 1×10^{-3} s^{-1}. Three tensile tests were performed with each sample and the average values were calculated. Vickers microhardness measurement was performed with Akashi microhardness tester. Electrical conductivity was measured using Sigmatest Foester.

Samples after casting and deformation were subjected to electrochemical corrosion test in artificial saliva. The corrosion test was carried out with the „Autolab" set – potentiostat/galvanostat from EcoChemie B.V. with GPES software ver. 4.9 for experiment control, data collection and analysis of results.

3. Results and discussion

Chemical compositions of the analyzed alloys are presented in Table 1.

In the microstructure of CuSn10, CuSn15 and CuSn20 alloys, the dendrites of α phase were observed. The interden-

TABLE 1

Chemical compositions of Cu-Sn alloys

	Copper wt.%	Tin wt.%
CuSn10	90,3%	9,70%
CuSn15	85,4%	14.6%
CuSn20	81,6%	18,4%

tritic regions consisted of eutectoid composition ($\alpha + \delta$ phase) (Figs. 2-4). Increase of tin content leads to increase of interdentritic regions and peritectic precipitates (Figs. 2-4).

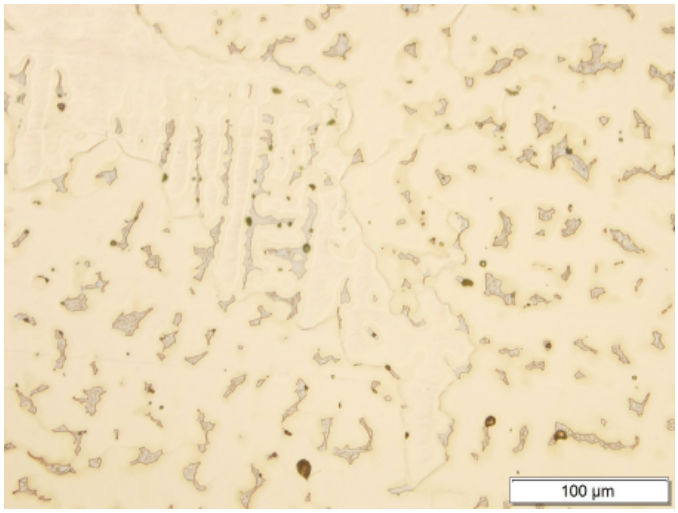

Fig. 2. Microstructure of CuSn10 alloy after casting and homogenization

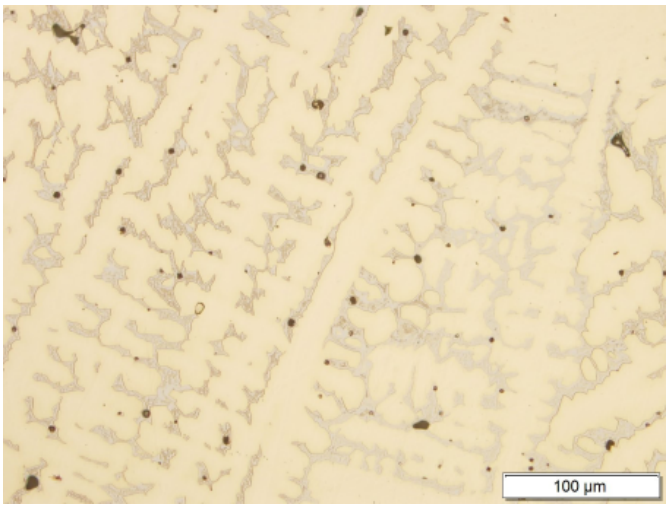

Fig. 3. Microstructure of CuSn15 alloy after casting and homogenization

The X-ray analysis showed presence of a copper-based solid solution α with a regular structure (Fm-3m space group) and an electron phase δ with a structure (F-43m space group). The δ phase is a solid solution based on the Cu31Sn8 electron phase of 21:13 electron concentration and cubic structure. In equilibrium conditions, this phase undergo eutectoid decomposition $\delta = \alpha + \varepsilon$ in a temperature of 350°C. A diffraction pattern of the CuSn15 alloy is shown in Fig. 5

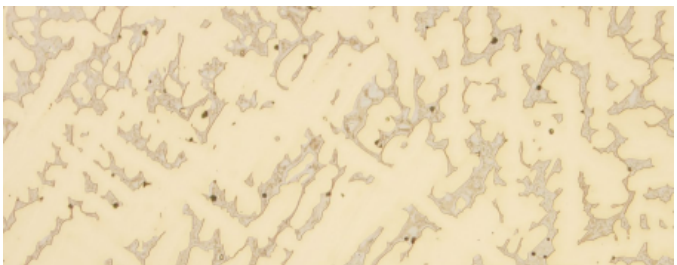

Fig. 4. Microstructure of CuSn20 alloy after casting and homogenization

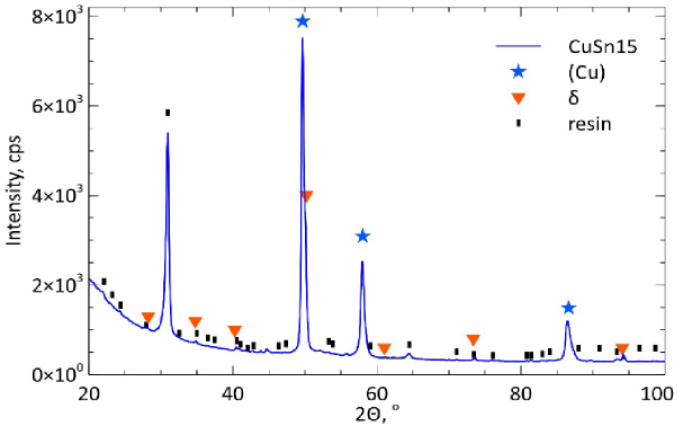

Fig. 5. Diffraction pattern of CuSn15 alloy

Microstructure observation of samples after KOBO processing showed presence of equiaxial grains of the α phase with twins and areas of the $\alpha + \delta$ eutectoid composition. The produced grains have a mean diameter significantly exceeding 1 µm (Figs. 6-8). From literature [14,17] it is known, that the formation of the twins is associated with the formation of stacking faults. During annealing, stacking faults are formed, which then grow continuously and finally transform to the nuclei of annealing twins.

The new fine-grained structure with twins, composed of α phase grains are well visible in STEM observations. A relatively small amount of dislocations are visible inside the new grains (Figs. 9-11). It should be noted, that independently of chemical composition of alloys, the effect of KOBO processing on creation of fine- microstructure is comparable.

The obtained results indicate that the KOBO deformation can lead to formation of a fine-grained structure. As a result of temperature increase resulting in deformation accumulation,

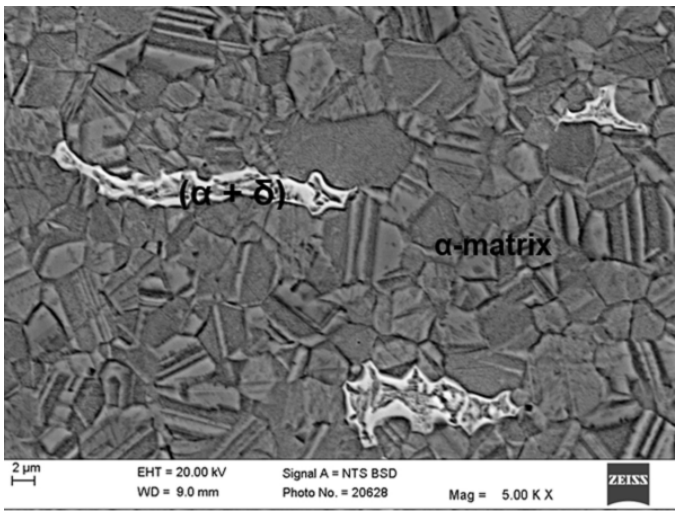

Fig. 6. Microstructure of CuSn10 alloy after KOBO, SEM

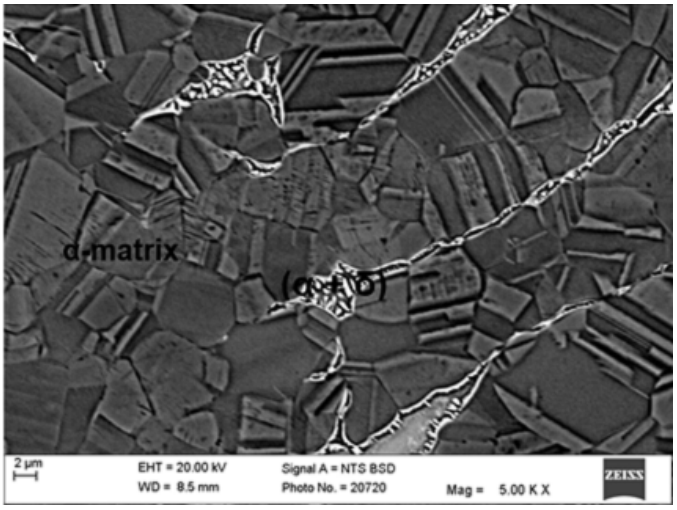

Fig. 7. Microstructure of CuSn15 alloy after KOBO, SEM

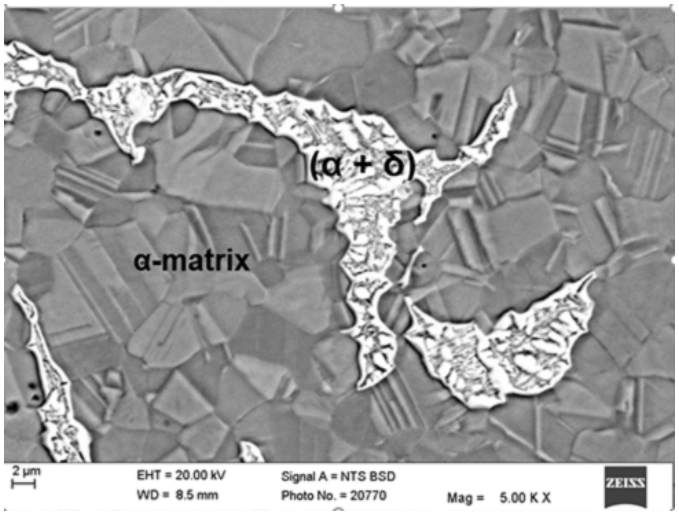

Fig. 8. Microstructure of CuSn20 alloy after KOBO, SEM

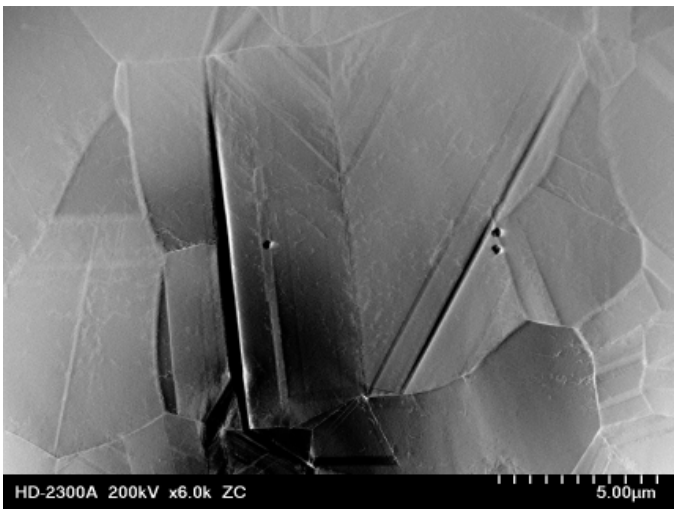

Fig. 9. Microstructure of CuSn10 alloy after KOBO, TEM

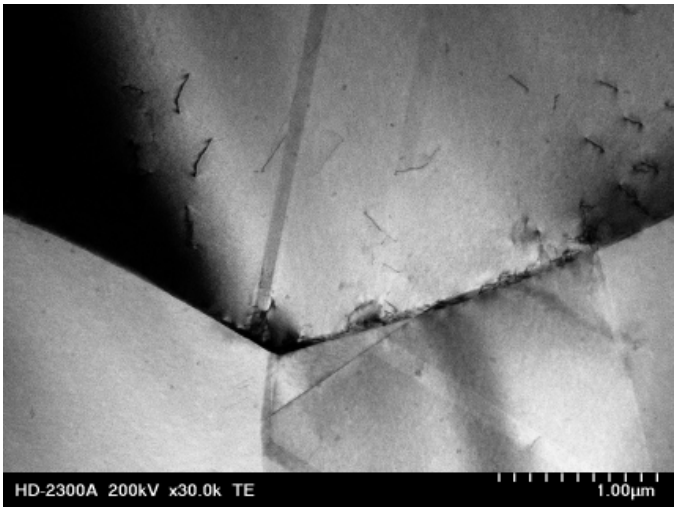

Fig. 10. Microstructure of CuSn15 alloy after KOBO, TEM

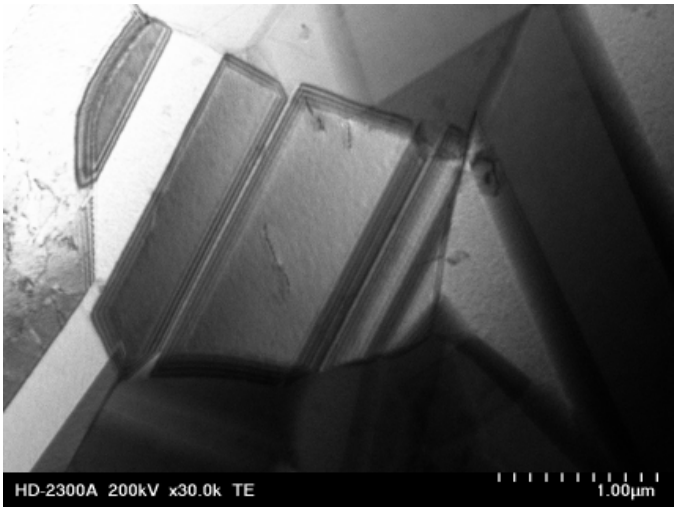

Fig. 11. Microstructure of CuSn20 alloy after KOBO, TEM

recrystallization processes take place, leading to formation of high angle boundaries with low dislocation density inside the new grains.

A lot of experiments showed that materials with low stacking fault energies, such as pure Cu and tin bronze are especially suitable for producing small grain sizes through SPD, although

the low rates of recovery lead to a slow evolution of the microstructure during processing [14]. This situation make easy to form recrystallized grains during deformation.

The example of interdendritic regions of the α phase are presented in (Figs. 12-13). The $\alpha + \delta$ morphology revealed by STEM did not show any differences between samples after casting and after KOBO. The shape of plates remained almost unchanged. After KOBO processing dislocation density increases in both phases.

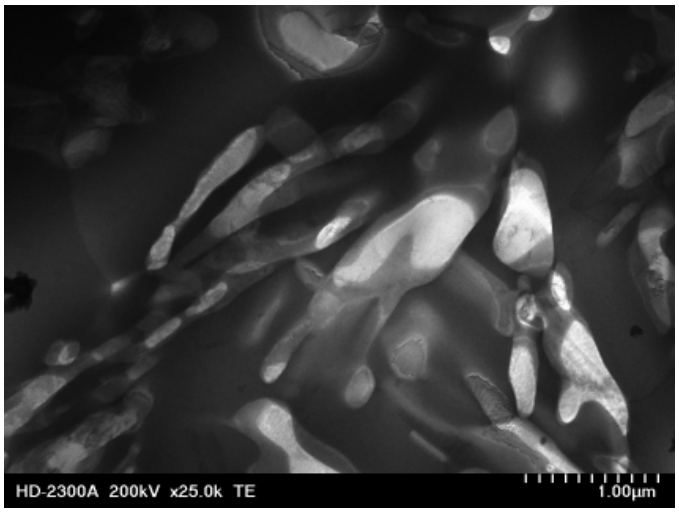

Fig. 12. Microstructure of CuSn20 alloy after casting

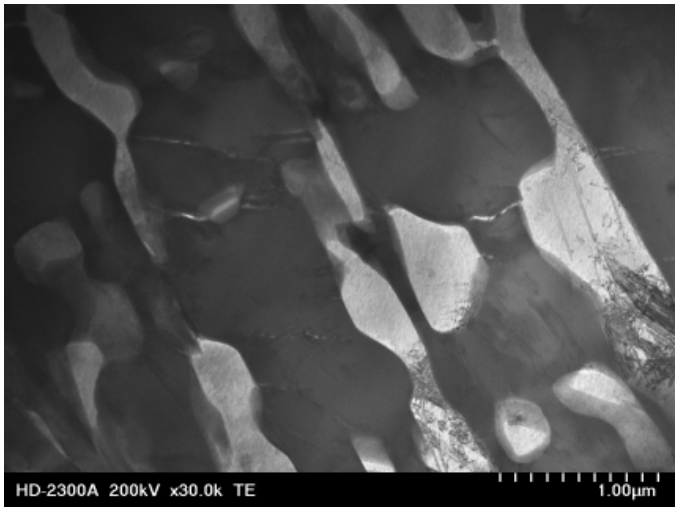

Fig. 13. Microstructure of CuSn20 alloy after KOBO processing

The Cu-Sn alloys were investigated with respect the changes in their mechanical properties. The mechanical properties of alloys after casting and KOBO deformation are shown in Table 2 and Table 3, respectively.

The KOBO deformation results in significant increase of hardness (HV), yield stress (YS) and ultimate tensile stress (UTS) compared with initial state after casting (Tables 2, 3). The hardness increases in Cu-Sn alloys with increasing of tin content (in CuSn20 alloy after KOBO processing the hardness was maximal). From Table 3 it can be seen that unlike the hardness, the strength properties do not increase with increase of tin content. Rather, there is a decrease in strength properties. Considerable improvement in strength values (both yield strength

TABLE 2

Mechanical properties of alloys: yield strength (YS), ultimate tensile strength (UTS), hardness (HV1), elongation ($A_5 = A_o - A/A_o$*100% where: A_o – initial diameter before deformation, A – diameter after deformation) of cast samples

Alloy	UTS [MPa] φ5	YS [MPa] φ5	A_5 [%]	HV1
CuSn10	286	174	14	94
CuSn15	280	157	9	132
CuSn20	198	147	4	136

TABLE 3

Tensile strength, yield strength, elongation and hardness of KOBO processed samples

Alloy	UTS [MPa] φ5	YS [MPa] φ5	A_5 [%]	HV1
CuSn10	593	313	16,3	161
CuSn15	584	262	14,1	164
CuSn20	562	248	12,8	170

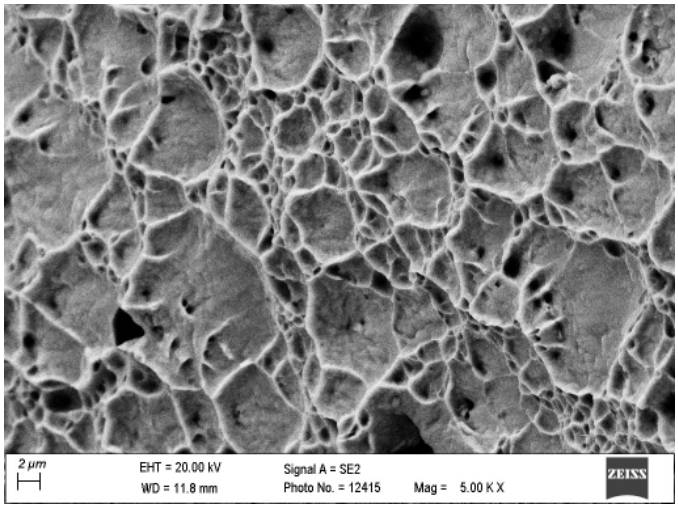

Fig. 14. Fracture surface of CuSn10 alloy after KOBO

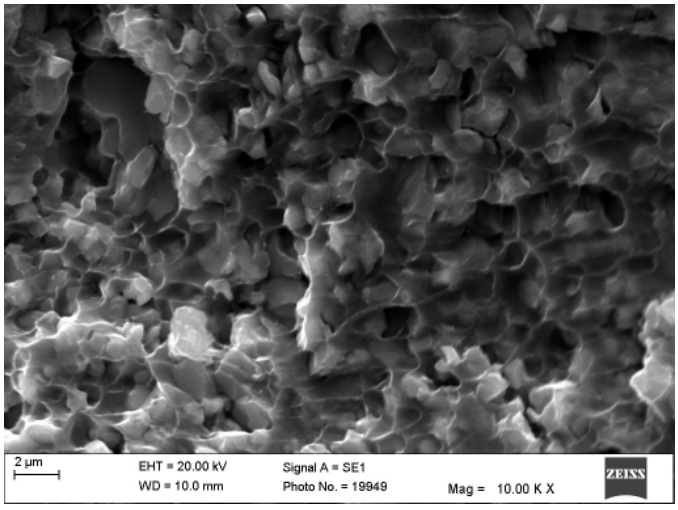

Fig. 15. Fracture surface of CuSn15 alloy after KOBO

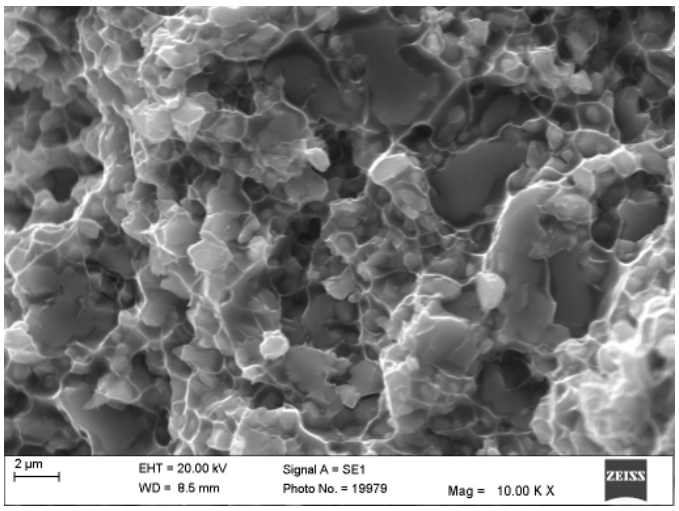

Fig. 16. Fracture surface of CuSn20 alloy after KOBO

and ultimate strength) are observed for CuSn10 alloy. For this alloy YS = 313 MPa and UTS = 593 MPa were reached. Gradual decrease of YS and UTS was reached for CuSn15 and CuSn20 alloys. The obtained results indicate that there exists a minimum Sn content in Cu-Sn alloy that is required for strength improvement to occur.

About two times (for CuSn10 and CuSn15) and about 2.8 times (for CuSn20) increase of UTS after KOBO processing compared to alloys after casting was reached.

Based on microstructure observation and strength properties measurements, it should be noted, that during deformation of Cu-Sn alloys by KOBO method the dislocation density and especially grain refinement will play important role in establishment of the relationship between the structure and strength properties. The tin content in Cu-Sn alloy played an important role in decrease of the strength properties. It was evident, that increase of tin reduces the YS and UTS effectively, as a results of presence of not tensile-resistant δ phase in structure. Tin content does not affect the grain size after KOBO deformation.

The maximum in ductility is observed in samples after KOBO deformation. This means that KOBO process is effective in ductility improvement. On the other hand, the presence of δ phase in alloys evidently decreases its ductility. A_5 for CuSn10 alloy after KOBO is 16.3%, while for CuSn20 alloy after deformation it is 12.8%.

The fracture surface analyses of the tensile tested samples after KOBO processing were conducted and representative images are shown in Figures 14-16. Under tensile loading, Cu-Sn alloys fracture exhibits dominant area at the base of the cup or cone. Cup and cone fracture occurs as a stepwise process characteristic for materials with moderately ductile failure [18-20]. There are, however, visible regions showing ductile character with characteristic "dimples" (Fig. 14-16). Regions with dimple-like ductile features were observed particularly in CuSn10 alloy (Fig. 14). The observed for CuSn15 and especially for CuSn20 alloy brittle mode of fracture is largely due to the presence of hard δ phase particles. Crack extension into matrix around debonded δ phase can be seen in Figure 16. In consequence, this can lead to low fracture strains. From obtained data it is evident that hard particles of δ phase acted as stress raisers and initiated void nucleation at the particle/matrix interface, resulting in debonding and alloy fracture.

It should be noted that in typically SPD processed materials decrease of ductility can be explained by reduction of mobility of dislocations due to considerable increase of dislocation density [1,2]. Meanwhile, in KOBO processed alloys the microstructure mainly consists of recrystalized grains which contain quite low-density dislocation.

For this reason mobility of dislocation is almost unrestricted. The obtained refined structure of α phase favours generation of high mechanical properties. In the presented study, the presence of hard δ phase in relatively softer α phase resulted in the reduction of ductility. This is due to the fact that these particles can act as local regions with high stress concentration which can initiate voids in the application of loads [20].

A literature review of Cu-Sn alloy indicates that research work on the SPD deformed alloy with comparable chemical composition has not been widely conducted, except in a few works only [15,16,22].

Conventionally, the cast materials provide improved strength properties at elevated temperatures. Most of the research works have reported such behaviour in Al and Mg based composites [20,21]. We believe that discussed in article alloys will show favourable mechanical properties at elevated temperature. It is planned to carry out such tests in the future.

Corrosion tests were performed using the electrochemical method in the environment of artificial saliva (Table 4), and showed that the increase of tin content results in increase of corrosion resistance. The values of the corrosion current density for the samples with a 20% Sn content are lower than 15% Sn, while the value of the polarization resistance is higher than 10%. However, no significant differences in the corrosion resistance between cast and KOBO processed materials were found. The addition of 15%wt. of Sn in cast materials results in reduction of corrosion potential to –400 mV from –287 mV as observed for 10% Sn content. In the KOBO processed materials the differences in the corrosion potential values are comparable with the state after casting.

TABLE 4

Chemical composition of artificial saliva

Component	Concentration [g/l]
Na_2HPO_4	1,3
NaCl	3,5
KSCN	1,65
K_2HPO_4	1,0
$NaHCO_3$	7,5
KCl	6,0

Table 5 presents results of electrochemical tests. Fig. 17 and Fig. 18 illustrate selected anodic polarization curves for samples after casting and for samples after KOBO, respectively.

TABLE 5

Results of electrochemical tests

Parameter / Sample	I_{corr} [μA/cm2]	E_{corr} [mV]	R_p [Ω]
Cast H10	12,23	–287	170,9
Cast H15	13,03	–400	88,89
Cast H20	3,663	–325	243,6
Extruded CuSn10H	7,955	–357	184,4
Extruded CuSn15H	15,35	–365	97,61
Extruded CuSn20H	5,971	–376	392,1

4. Conclusions

Cu-Sn alloys with different Sn contents were produced using KOBO technique. The alloys after deformation were evaluated to determine their microstructure and mechanical properties. The main results can be summarized as follows:

1. In the microstructure of CuSn10, CuSn15 and CuSn20 alloys, the dendrites of α phase were observed. The interdentritic regions consisted of eutectoid composition ($\alpha + \delta$ phase). The content of composition ($\alpha + \delta$ phase) increased with tin increase.
2. The obtained results showed possibility of KOBO deformation of CuSn10, CuSn15, CuSn20 casting alloys. KOBO processing contributed to the refinement of grains.
3. KOBO processed Cu-Sn alloys consist of equiaxial recrystallized grains with large amounts of twins. The grain size is above 1 μm, regardless of alloy composition.
4. The $\alpha + \delta$ phases morphology remained almost unchanged after KOBO deformation.
5. KOBO processing is required to improve mechanical properties of alloy. The strength properties as YS is about 1.6 times higher than in samples after casting. Improvement in yield stress was attributed to grain boundary strengthening and dislocation strengthening.
6. The addition of tin slightly improved the hardness. Meanwhile, with the increase of tin content, the tensile strength UTS and yield strength YS of alloys decrease gradually.
7. Eutectoid composition and especially δ phase control ductility properties, because of initiation of nucleation of void at the particle/matrix interface.
8. Corrosion tests performed using the electrochemical method in the environment of artificial saliva showed that the increase of tin content results in increase of corrosion resistance

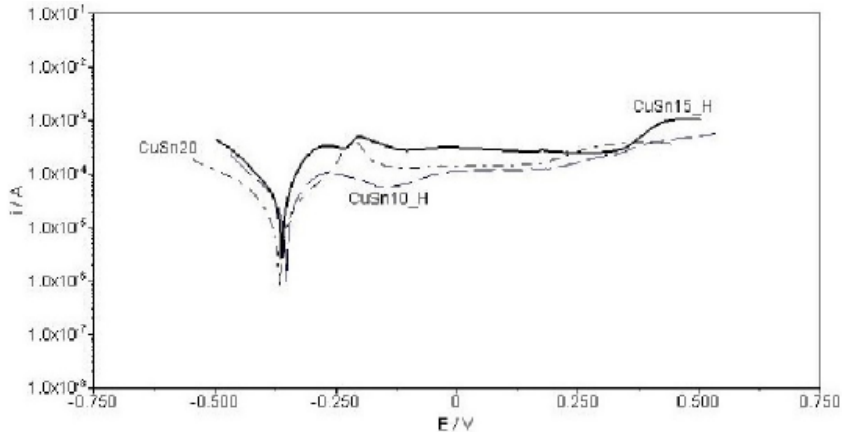

Fig. 17. Polarization curves of CuSn10 H, CuSn15 H, CuSn20 H cast samples

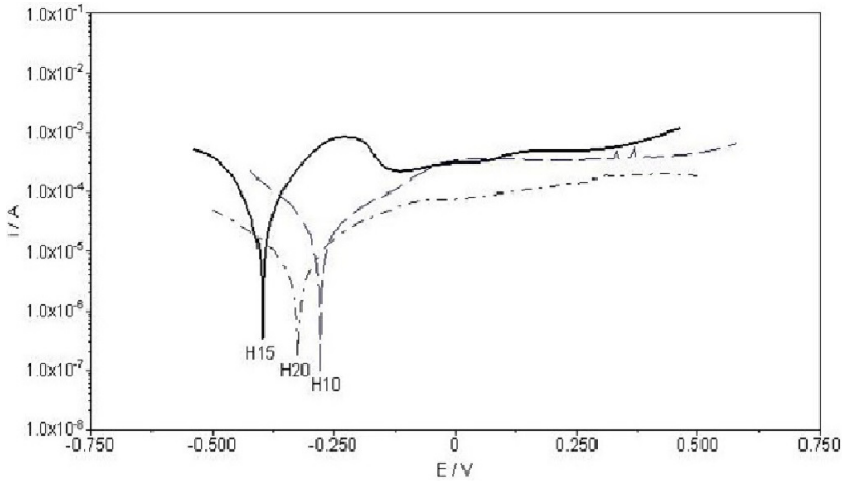

Fig. 18. Polarization curves of CuSn10 (H10), CuSn15 (H15), CuSn20 (H20) KOBO processed samples

Acknowledgment

The study was conducted within the scope of Statutory Work of Institute of Non-Ferrous Metals "Development of basic engineering for production of tin bronze rods with increased tin content using severe plastic deformation".

REFERENCES

[1] I.V. Alaxandrov, R.Z. Valiev, Scripta Mater. **44**, 1605-1608 (2001).
[2] P.B.Prangnell, J.R.Boven, Gholinia A. International Symposium on Materials Science DK: Risø,105-126 (2001).
[3] A. Neishi, T. Uchida, A. Yamauchi, K. Nakamura, Z. Horita, T.G. Langdon, Mate. Sci. and Engineering **A307**, 23-28(2001).
[4] R.Z. Valiev, O.A. Kaibyshev, R.I. Kuznetsov, R.Sh. Musalimov, N.K. Tsenev, Dokl. Akad. Nauk SSSR **301**, 964 (1988).
[5] W. Bochniak, Teoretyczne i praktyczne aspekty plastycznego kształtowania metali. Metoda KoBo, Kraków, Wyd. AGH 2009.
[6] J. Kawałko, P. Bobrowski, P. Koprowski, A. Jastrzębska, M. Bieda, M. Ładoga, K. Sztwiertnia, Journal of Alloys and Compounds **707**, 298-303 (2017).
[7] A. Korbel, J. Pospiech, W. Bochniak, A. Tarasek, P. Ostachowski, J. Bonarski, Int. J. Mater. Res. **102**, 464-473 (2011).
[8] L.X. Kong, P.D. Hodgson, Mater. Sci. Eng. A **308**, 209-215 (2001).
[9] D. Orlov, Y. Todaka, M. Umemoto, N. Tsuji, Mat. Sci. and Eng. A **499**, 427-433 (2009).
[10] I. Sabirov, M.Y. Murashkin, R.Z. Valiev, Mater. Sci. Eng. A 5**60**,-1-24 (2013).
[11] A. Vinogradov, T. Ishida, K. Kitagawa, V.I. Kopylov, Acta Mater. **53**, 2181-2192 (2005).
[12] W. Huang, L. Chai, Z. Li, X. Yang, N. Guo, B. Song, Materials Characterization **114**, 204-210 (2016).
[13] X. Chen, Z. Wang, D. Ding, H. Tang, L. Qiu, X. Luo, G. Shi, Materials and Design **66**, 60-66 (2015).
[14] J. Hui, Z. Feng, W. Fan, X.Yuan, Materials Charakteryzation **144**,611-620, (2018).
[15] A. Korneva, B. Straumal, A. Kilmametov, L. Lityńska-Dobrzyńska, G. Cios, P. Bała, P. Zięba, Mater. Charact. **118**, 411-416 (2016).
[16] A. Korneva, B. Straumal, R. Chulist, A. Kilmametov, P. Bała, G. Cios, N. Schell Mat. Lett. **179**, 12-15 (2016).
[17] R. Gupta, S. Srivastava, N. Kishor Kumar, S.K. Panthi, Materials Science &Engineering A **654**, 282-291 (2016).
[18] J. Subramanian, Z. Loh, S. Seetharaman, Abdelmagid S. Hamouda, M. Gupta, Metals **2**, 178-194 (2012).
[19] T.C. Tszeng, Composites B **29B**, 299-308 (1998).
[20] K. Purazrang, K.U. Kainer, B.L. Mordike, Composites **22**, 456-460 (1991).
[21] N.J Musson, T.M. Yue, The effect of matrix composition on the mechanical properties of squeeze-cast aluminium alloy-Saffil metal matrix composites, Mater. Sci. Eng. A **135**, 237-242 (1991).
[23] B. Alili, D. Bradai, P. Zieba, Materials Charakterization **59**, 1526-1530 (2008).
[23] W. Głuchowski, Z. Rdzawski, J. Sobota, J. Domagała-Dubiel, Arch. Metall. Mater. **61** (2B), 1207-1214 (2016).
[24] K. Rodak, J. Sobota, W. Głuchowski, Mater. Sci. Forum **890** (1662-9752), 327-330 (2017)